Chinese Chemical Letters 37 (2026) 111446

Contents lists available at ScienceDirect

Chinese Chemical Letters

journal homepage: www.elsevier.com/locate/cclet

Asymmetric bioactive phosphorus dendrimers deliver bromelain for enhanced anti-inflammation and chondroprotection therapy of osteoarthritis

Huxiao Sun[a,1], Jin Li[a,1], Mengsi Zhan[a], Yu Zou[a,*], Caiyun Zhang[a], Serge Mignani[b,c], Regis Laurent[d,e], Jean-Pierre Majoral[d,e], Xiangyang Shi[a,b,*], Mingwu Shen[a,*]

[a] State Key Laboratory of Advanced Fiber Materials, Shanghai Engineering Research Center of Nano-Biomaterials and Regenerative Medicine, College of Biological Science and Medical Engineering, Donghua University, Shanghai 201620, China
[b] CQM-Centro de Química da Madeira, Universidade da Madeira, Campus Universitário da Penteada, Funchal 9020-105, Portugal
[c] Centre d'Etudes et de Recherche sur le Medicament de Normandie (CERMN), Université de Caen Normandie, Caen 14032, France
[d] Laboratoire de Chimie de Coordination du CNRS, 205 Route de Narbonne, CEDEX 4, Toulouse 31077, France
[e] Université Toulouse, 118 Route de Narbonne, CEDEX 4, Toulouse 31077, France

ARTICLE INFO

Article history:
Received 23 March 2025
Revised 8 June 2025
Accepted 10 June 2025
Available online 11 June 2025

Keywords:
Phosphorus dendrimer
Bromelain
Macrophage M2 polarization
Anti-inflammation
Osteoarthritis

ABSTRACT

It is still challenging to develop nanomedicines with full-active and simple components to tackle osteoarthritis (OA) through restoration of inflammation and cartilage homeostasis. Here, we report the synthesis of a bioactive asymmetric phosphorus dendrimer bearing an azabisphosphonate (ABP) group, termed as G0.PD-ABP, by a divergent method for intracellular bromelain (Bro) delivery. The formed G0.PD-ABP/Bro nanocomplexes (NCs) exhibit a uniformly dispersed spherical shape with a mean size of 148.4 nm and can achieve more significant intracellular Bro delivery than symmetric phosphorus dendrimer (G0.PD) without ABP *via* the clathrin-mediated endocytosis pathway. Importantly, the NCs efficiently block the activation of inducible nitric oxide synthase (iNOS), cyclooxygenase-2 (COX-2), and nuclear factor kappa-B (NF-κB) by amplifying the anti-inflammatory function of Bro and synergizing with the immunomodulatory activity of dendrimers, thereby facilitating the polarization of macrophages towards M2 phenotype and down-regulating inflammatory cytokine secretion to lead to suppressed chondrocyte apoptosis. Compared with G0.PD/Bro NCs, an OA mouse model treated with G0.PD-ABP/Bro NCs demonstrates more remarkable alleviation of pathological features such as cartilage degradation, bone erosion, and synovial inflammation. This study emphasizes the positive contribution of structural asymmetry of phosphorus dendrimers in protein delivery and provides a viable strategy for the treatment of OA or other inflammatory diseases through enhanced immune modulation of macrophages.

© 2025 Published by Elsevier B.V. on behalf of Chinese Chemical Society and Institute of Materia Medica, Chinese Academy of Medical Sciences.

Osteoarthritis (OA), a chronic degenerative disease, is distinguished by persistent inflammation and cartilage deterioration, ultimately culminating in cartilage lesions and subchondral bone abnormalities [1]. Pharmaceutical interventions advocated by clinical guidelines predominantly include analgesic and anti-inflammatory drugs, such as paracetamol and nonsteroidal anti-inflammatory drugs (NSAIDs) [2]. However, these interventions exhibit limited efficacy in slowing down the progression of OA and possess the potential gastrointestinal toxicity [3,4]. Total joint-replacement surgery, as a common clinical surgical treatment of advanced OA, may be risky due to various postoperative complications and lead to a heavy personal financial burden [5]. Therefore, there is an urgent requirement to develop safe and efficient management strategies for OA.

Articular cartilage tissue in OA patients undergoes uncontrolled malignant degradation. Therefore, various therapeutic strategies with the function of inhibiting chondrocyte apoptosis [1,6], improving chondrocyte anabolism [7], maintaining chondrocyte phenotype [8], inducing chondrogenic differentiation of bone marrow mesenchymal stem cells [9], and reducing cartilage wear [10] have been developed to protect or regenerate cartilage tissue. However, synovitis triggered by continuous inflammation is another crucial pathologic characteristic that should not be neglected.

* Corresponding authors.
E-mail addresses: yuzou@dhu.edu.cn (Y. Zou), xshi@dhu.edu.cn (X. Shi), mwshen@dhu.edu.cn (M. Shen).
[1] These authors contributed equally to this work.

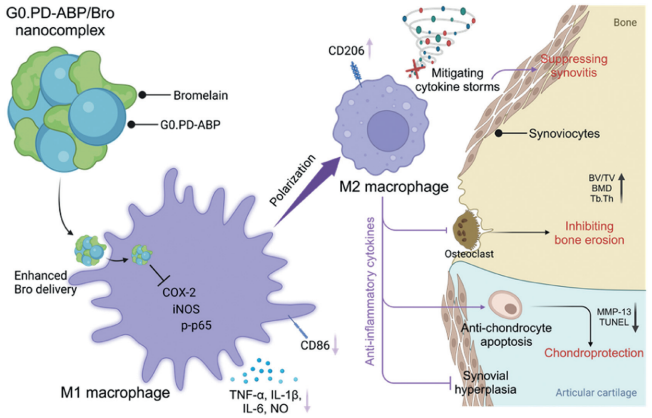
https://doi.org/10.1016/j.cclet.2025.111446
1001-8417/© 2025 Published by Elsevier B.V. on behalf of Chinese Chemical Society and Institute of Materia Medica, Chinese Academy of Medical Sciences.

Macrophages, the most abundant immune cells in the synovium, influence various cellular responses and biological processes by switching immune phenotypes between M1 and M2 [11]. In this case, overactivated synovial macrophage (M1-type) dominate the secretion of many proinflammatory cytokines and catabolic factors, including tumor necrosis factor-α (TNF-α), cyclooxygenase-2 (COX-2), inducible nitric oxide synthase (iNOS), prostaglandin E2 (PGE2), and matrix metalloproteinases (MMPs) at the joint site [12]. The production of these mediators exacerbates OA progression by inducing the extracellular matrix (ECM) degradation and chondrocyte dysfunction [13]. Consequently, comprehensive treatment of OA may be achieved by polarizing activated macrophages to reduce inflammatory cytokine secretion through immune microenvironment modulation [14,15].

Bromelain (Bro), a natural product derived from pineapple rhizomes, has been employed to treat different inflammatory diseases such as OA, rheumatoid arthritis and asthma with excellent biosafety [16]. Bro possesses powerful anti-inflammatory effects and macrophage polarization capabilities by inhibiting nuclear factor kappa B (NF-κB) and mitogen-activated protein kinases (MAPKs) signaling pathways in macrophages [17]. Meanwhile, Bro can also block the conversion of arachidonic acid into prostaglandins through the regulation of COX-2 expression to exert analgesic effect [18]. The biological activity of Bro holds great promise for the treatment of OA. However, the membrane impermeability of Bro resulting from its high molecular weight and hydrophilicity leads to its difficulty to be phagocytosed by target cells, thereby exhibiting limited activity within organisms. Nanocarrier-based cytoplasmic protein delivery technologies, including dendrimers [19], supramolecules [20], polymers [21,22], and nanogels [23], offer opportunities for the development of protein therapeutics. However, these nanocarriers typically incorporate high-density positive charges that may raise biosafety concerns [24], and simultaneously overlook the carriers' potential for directly modulating disease processes [25]. Therefore, the rational design of non-cationic nanocarriers with intrinsic bioactivity and efficient protein delivery capability is essential for augmenting disease therapeutic efficacy through the function synergy of the carrier and delivered substance.

Several non-cationic phosphorus dendrimers with macrophage polarization and natural killer cell proliferation properties have been reported to serve as efficient and safe carriers for intracellular protein delivery [26,27]. Especially, phosphorus dendrimers terminated with phosphonate or hydroxyl groups can amplify the biological activity of the delivered proteins while synergizing their inherent anti-inflammatory activity [15,26,28]. Because asymmetric cationic phosphorus dendrimers exhibit superior and unimpaired gene compression and delivery properties [29], we hypothesize that the structural asymmetry of anionic phosphorus dendrimers may affect intracellular protein delivery efficiency, thereby improving disease therapeutic outcomes. As a result, the utilization of asymmetric bioactive phosphorus dendrimers to deliver Bro may represent a rational design for enhanced OA treatment.

In this study, we employed an anionic asymmetric phosphorus dendrimer as an intracellular delivery carrier of Bro to polarize macrophage towards M2 phenotype for enhanced anti-inflammatory and chondroprotection treatment of OA. Firstly, asymmetric phosphorus dendrimers bearing with azabisphosphonate (ABP) group, termed as G0.PD-ABP, were synthesized using a divergent method. The differences in anti-inflammatory activity and protein delivery properties between G0.PD-ABP and G0.PD (a symmetric phosphorus dendrimer without ABP group) were investigated. Then, the synergistic anti-inflammation and anti-chondrocyte apoptosis ability of Bro delivery mediated by G0.PD-ABP was systematically investigated *in vitro* and *in vivo* using an OA mouse model (Scheme 1). The significant characteristics of this



Scheme 1. Schematic diagram of G0.PD-ABP/Bro for anti-inflammatory and chondroprotective treatment of OA.

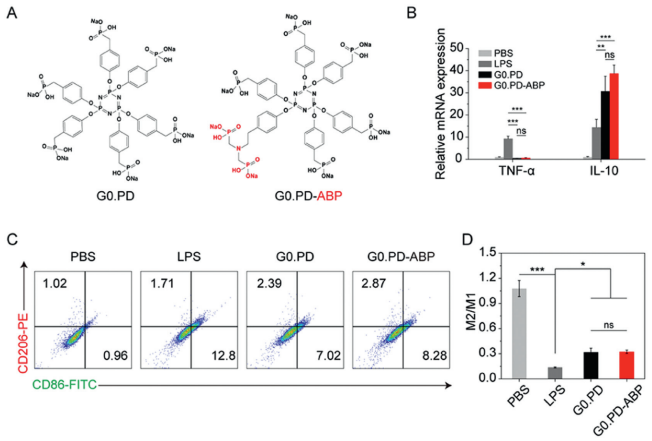


Fig. 1. Anti-inflammatory activity of G0.PD and G0.PD-ABP. (A) Chemical structure of G0.PD and G0.PD-ABP. (B) mRNA expression levels of TNF-α and IL-10 in activated RAW264.7 cells after treated with G0.PD or G0.PD-ABP for 24 h. (C) Flow cytometry analysis of macrophage polarization in activated RAW264.7 cells treated with G0.PD or G0.PD-ABP for 24 h. (D) The quantitation of M2/M1 ratio after RAW264.7 cells were exposed to G0.PD or G0.PD-ABP for 24 h. Data are presented as mean ± standard deviation ($n = 3$). ns, no significance. $^{*}P < 0.05$, $^{**}P < 0.01$, $^{***}P < 0.001$.

study are as follows: (1) To elucidate the contribution of structural asymmetry of phosphorus dendrimers in protein delivery; (2) to enhance the intracellular delivery efficiency of Bro through the utilization of G0.PD-ABP; (3) to integrate the inherent immunomodulation properties of G0.PD-ABP and Bro to achieve efficient anti-inflammatory and anti-chondrogenic apoptotic therapy of OA.

The protein delivery capabilities and immunomodulatory effects of phosphorus dendrimers terminated with phosphonate groups have been extensively verified [30]. However, the impact of the structural symmetry of phosphorus dendrimers on the efficiency of intracellular protein delivery and inherent biological functionalities remain to be investigated since the symmetry of the phosphorus dendrimers is expected to have direct impact on their molecular rigidity and protein delivery efficiency. Therefore, an asymmetric phosphorus dendrimer (G0.PD-ABP) was synthesized using a divergent iterative method (Fig. S1 in Supporting information). The chemical structures of G0.PD-ABP and the control compound G0.PD (symmetric phosphorus dendrimer) are shown in Fig. 1A. ^{1}H and ^{31}P nuclear magnetic resonance (NMR) spectra were adopted to characterize all the intermediates and final products (Figs. S2–S8 in Supporting information).

In anti-inflammation activity profile, G0.PD and G0.PD-ABP all significantly downregulate the messenger ribonucleic acid (mRNA)

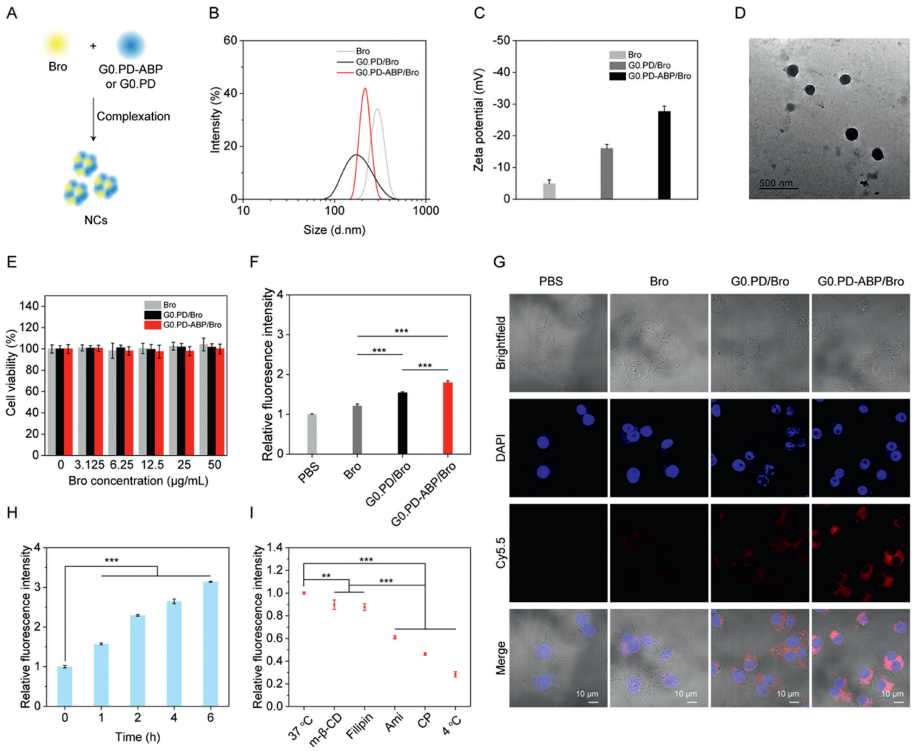


Fig. 2. Phosphorus dendrimer/Bro NCs improve the efficiency of intracellular Bro delivery. (A) Phosphorus dendrimers complexed with Bro to form the NCs. (B) Hydrodynamic size distributions and (C) zeta potentials of Bro, G0.PD/Bro, and G0.PD-ABP/Bro. (D) TEM image of G0.PD-ABP/Bro NCs. (E) Viability of activated RAW264.7 cells treated with Bro, G0.PD/Bro or G0.PD-ABP/Bro at different Bro concentrations ($n = 5$). (F) Relative fluorescence intensity of activated RAW264.7 cells treated with PBS, Bro, G0.PD/Bro or G0.PD-ABP/Bro (Bro was labeled with Cy5.5) for 4 h. (G) CLSM images of activated RAW264.7 cells after different treatments for 4 h. (H) Relative fluorescence intensity of activated RAW264.7 cells after treatment with G0.PD-ABP/Bro for different time periods. (I) Relative fluorescence intensity of activated RAW264.7 cells treated with G0.PD-ABP/Bro for 4 h. The cells were pretreated with different inhibitors for 2 h before materials incubation. In panels C, F, H, and I, $n = 3$. Data are presented as mean ± standard deviation. $^{**}P < 0.01$, $^{***}P < 0.001$.

expression levels of proinflammatory cytokines TNF-α and upregulate the mRNA expression levels of anti-inflammatory interleukin (IL)-10, but the symmetry of the phosphorus dendrimers does not seem to significantly affect their intrinsic anti-inflammatory activity (Fig. 1B). Flow cytometry analysis was also performed to investigate the expression of biomarkers associated with macrophage polarization in activated RAW264.7 cells following different treatments. Lipopolysaccharide (LPS), as an agonist of Toll-like receptors, can induce macrophage polarization toward M1-phenotype (Fig. 1C). Since the modification of phosphate on the surface of phosphorus dendrimer elicits a unique capacity for macrophage polarization, treatments with G0.PD and G0.PD-ABP exhibit a profound impact on macrophage phenotype, specifically by inhibiting the expression of M1 biomarker cluster of differentiation (CD) 86 and increasing the population of CD206 positive macrophages (Fig. S9 in Supporting information). Although G0.PD and G0.PD-ABP significantly increase the M2/M1 ratio by 2.32- and 2.38-fold compared with the LPS group ($P < 0.05$), respectively, no significant difference is observed between these two types of dendrimers (Fig. 1D). This further suggests that the structural symmetry does not play a role in enhancing the immunomodulatory activity of phosphorus dendrimers.

To explore the contribution of the structural symmetry of phosphorus dendrimers to intracellular protein delivery efficiency, G0.PD or G0.PD-ABP dendrimers were respectively complexed with protein Bro to obtain stable G0.PD/Bro or G0.PD-ABP/Bro nanocomplexes (NCs) (Fig. 2A). Dynamic light scattering (DLS) analyses reveal that both G0.PD/Bro and G0.PD-ABP/Bro NCs exhibit uniform hydrodynamic size distributions with the mean sizes of 190.7 and 217.5 nm, respectively (Fig. 2B), which are smaller than naked Bro (298.2 nm). Moreover, the surface potentials of G0.PD/Bro and G0.PD-ABP/Bro NCs decrease from −4.9 mV of Bro to −16.1 and −27.7 mV, respectively (Fig. 2C). This implies that the two phosphorus dendrimers achieve effectively complexation with Bro through simple physical interactions. However, the protein encapsulation efficiency of G0.PD-ABP (72.3 %) with asymmetric structure is higher than that of symmetric G0.PD (53.0 %), reflecting an enhancement in protein complexation ability of phosphorus dendrimer upon the introduction of ABP cap. This is further corroborated by the deeper Bro characteristic bands observed in the sodium dodecyl sulfate-polyacrylamide gel electrophoresis (SDS-PAGE) image of the G0.PD-ABP/Bro group than that of the G0.PD/Bro group (Fig. S10). The stronger protein binding capacity of G0.PD-ABP than that of G0.PD may be due to the presence of an additional phosphate group and a nitrogen atom in the G0.PD-ABP dendrimer, which enhances the electrostatic and hydrogen bonding interactions between G0.PD-ABP and Bro [31,32]. Additionally, transmission electron microscopy (TEM) image reveals that the sizes of the G0.PD/Bro and G0.PD-ABP/Bro NCs are about 137.4 and 148.4 nm, respectively (Fig. 2D and Fig. S11 in Supporting information). Notably, the G0.PD-ABP/Bro NCs exhibit a more uniformly dispersed and compact spherical morphology than the G0.PD/Bro NCs, further indicating that the structural asymmetry may impart improved protein compression and packing effects to phosphorus dendrimers. Isothermal titration calorimetry (ITC) results reveal the presence of two binding sites between G0.PD-ABP and Bro (Table S2 and Fig. S12 in Supporting information). The significantly higher binding constant (K_a) of site 1 than that of site 2 indicates a stronger binding affinity at site 1. This interaction at site 1 is mainly an exothermic process driven by electrostatic interaction, hydrogen bonding, and van der Waals force as evidenced by the thermodynamic parameters exhibiting enthalpy change (ΔH)

< 0 and entropy change (ΔS) < 0 [33,34]. Conversely, positive thermodynamic parameters suggest that the interaction at site 2 is mediated by hydrophobic interaction [35]. Taken together, the complexation between the G0.PD-ABP and Bro represents a multifaceted process involving multiple physical interactions.

The cell counting kit (CCK)-8 experiment reveals that the G0.PD/Bro and G0.PD-ABP/Bro NCs possess outstanding cytocompatibility and the viability of LPS-activated macrophages treated with the NCs remains above 90% even at a Bro concentration of 50 μg/mL (Fig. 2E). It seems that the cytocompatibility of free Bro is not compromised when complexed with both types of dendrimers. Considering the favorable anti-inflammatory activity of Bro against activated macrophages at concentrations ranging from 20 μg/mL to 40 μg/mL [17], 30 μg/mL of Bro was selected as the effective concentration for subsequent *in vitro* experiments. Subsequently, we explored the effects of intracellular Bro delivery of both NCs using flow cytometry and confocal laser scanning microscopy (CLSM). The inadequate membrane permeability of Bro significantly impedes its effectiveness in cytoplasmic delivery (Fig. 2F). Conversely, the robust protein delivery capability of phosphorus dendrimers facilitates an augmented Bro delivery efficiency, which is visually demonstrated by a uniformly dispersed red fluorescent signal observed in both the G0.PD/Bro and G0.PD-ABP/Bro groups (Fig. 2G). Furthermore, the fluorescence intensity of RAW264.7 cells treated with G0.PD-ABP/Bro NCs is significantly higher than that of the G0.PD/Bro group (Figs. 2F and G), potentially attributed to the structural asymmetry induced by the incorporation of ABP to facilitate enhanced binding efficacy between dendrimers and proteins.

Considering that G0.PD-ABP has better intracellular Bro delivery effect, we then investigated the phagocytic pathways of G0.PD-ABP/Bro in LPS-activated macrophages. As illustrate in Fig. 2H and Fig. S13A (Supporting information), the G0.PD-ABP/Bro NCs can be phagocytosed by activated macrophages in a time-dependent manner. Meanwhile, pretreatments with methyl-β-cyclodextrin (m-β-CD) and filipin only modestly reduce the cellular uptake of G0.PD-ABP/Bro NCs, exhibiting substantially weaker inhibitory effects compared to the chlorpromazine (CP) and amiloride (Ami) pretreatment groups (Fig. 2I). This indicates that most of NCs are internalized predominantly *via* clathrin- and micropinocytosis-mediated endocytosis pathways, rather than lipid raft- or caveolae-mediated mechanisms. Additionally, low temperature exerts an inhibitory effect on the phagocytic capability of macrophages against G0.PD-ABP/Bro, suggesting that an adequate energy supply is indispensable for the cellular internalization of G0.PD-ABP/Bro NCs (Fig. S13B in Supporting information).

Abnormal activation of synovial macrophages is an important factor involved in the progression of OA [36]. Considering the inherent immunomodulatory properties of both Bro and G0.PD-ABP, we subsequently embarked to elucidate the potential of G0.PD-ABP to amplify the anti-inflammatory activity of Bro by enhancing the intracellular Bro delivery (Fig. 3A). Despite a significant increase in the proportion of CD86 positive macrophages (M1) following LPS challenge, treatment with G0.PD/Bro or G0.PD-ABP/Bro triggers a significant reduction in the percentage of M1 macrophages, with the reduction being superior to that achieved by free Bro (Fig. 3B, $P < 0.001$). Importantly, the G0.PD-ABP/Bro group exhibits a markedly elevated proportion of CD206-positive macrophages (M2, 15.7%) compared to the G0.PD/Bro group (11.6%, $P < 0.01$). This finding indicates that the G0.PD-ABP/Bro NCs display a powerful macrophage M2-type polarization ability by synergizing the improved Bro delivery with the immunomodulatory activity *per se* of dendrimers (Fig. 3C).

Next, the expression levels of typical inflammatory cytokines (including TNF-α, IL-1β, and IL-6) were evaluated to reflect the anti-inflammatory response of NCs in activated macrophages. An intensive inflammatory response is observed in LPS-treated RAW264.7 cells with the dramatically enhanced IL-1β, IL-6, and TNF-α levels (Fig. 3D and Fig. S14 in Supporting information). However, Bro alone has limited efficacy in reducing the expression of LPS-induced proinflammatory cytokines due to its poor membrane permeability. Fortunately, the G0.PD-ABP/Bro NCs significantly suppress the expression of various pro-inflammatory cytokines while concurrently promote the secretion of anti-inflammatory cytokine IL-10, thereby highlighting their potent inflammatory modulation efficacy (Fig. 3D). The downregulation of TNF-α mRNA and the upregulation of IL-10 mRNA mediated by the G0.PD-ABP/Bro NCs further support the contention that intracellular Bro delivery facilitated by G0.PD-ABP exerts synergistic anti-inflammatory properties (Fig. S15 in Supporting information). Subsequently, we identify that G0.PD-ABP/Bro NCs possess the capability to interfere with the synthesis process of intracellular nitric oxide (NO) (Fig. 3E), a mediator implicated in the disruption of mitochondrial respiration and exacerbation of inflammatory response [37,38]. This inhibitory effect is predominantly ascribable to the ability of G0.PD-ABP/Bro to suppress the expression of inducible nitric oxide synthase (iNOS) (Fig. 3F and Fig. S16A in Supporting information). Moreover, Bro blocks prostaglandin production by inhibiting COX-2 expression to relieve inflammation and reduce OA patients' sensitivity to pain (Fig. 3F). Importantly, both dendrimers, particularly G0.PD-ABP, significantly amplify the inhibitory effect of Bro on COX-2 through improved intracellular Bro delivery (Fig. S16B in Supporting information). Since phosphorus dendrimers modified with phosphate are widely reported to suppress nuclear factor-kappa B (NF-κB) inflammatory signaling pathway [39], we show that the G0.PD-ABP/Bro NCs significantly down-regulate the expression of p-p65 (Fig. S16C in Supporting information). This observation may elucidate an important molecular mechanism underlying the potent anti-inflammatory activity of G0.PD-ABP/Bro NCs. Specifically, G0.PD-ABP/Bro NCs intervene in the activation of intracellular key inflammatory signaling pathways (including iNOS, COX-2, and NF-κB) by enhancing the intracellular Bro delivery and synergistically integrating the intrinsic immunomodulatory activity of both Bro and the G0.PD-ABP dendrimer.

Activated macrophages can proliferate rapidly in pathological environments and release inflammatory mediators, resulting in chondrocyte apoptosis and cartilage destruction [40]. Consequently, the ability of G0.PD-ABP/Bro NCs to inhibit inflammation-induced death of chondrocytes was evaluated by co-culture chondrocytes with different conditional media (CM, supernatant from macrophages treated with different materials). The Annexin V-FITC/PI co-staining assay confirms that CM from LPS-activated macrophages results in 18.9% of chondrocytes to undergo apoptosis and necrosis. In contrast, CM derived from macrophages treated with either Bro or G0.PD/Bro significantly decreases the chondrocyte apoptosis/necrosis percentage (Fig. 3G). Importantly, the apoptotic state of chondrocytes induced by inflammatory mediators is nearly reversed and restored to normal levels following treatment with CM in the G0.PD-ABP/Bro group (Fig. 3H), which indicates the effective chondroprotective ability of G0.PD-ABP/Bro by exerting the best anti-inflammatory and macrophage M2 polarization properties among all studied materials.

To validate the anti-inflammatory and chondroprotective therapeutic effects of G0.PD-ABP/Bro *in vivo*, BALB/C mice were used to establish a knee OA model and treated with different materials (Fig. 4A). All animal experiments were performed in accordance with the approved guidelines of the Committee on Experimental Animal Care and Use of Donghua University (approval No DWSY202410240146). The *in vivo* dosage of G0.PD-ABP/Bro NCs was determined based on our earlier studies using a protein drug for OA treatment [15]. The knee joint of each mouse was initially collected to perform safranin O/fast green (SO-FG) stain-

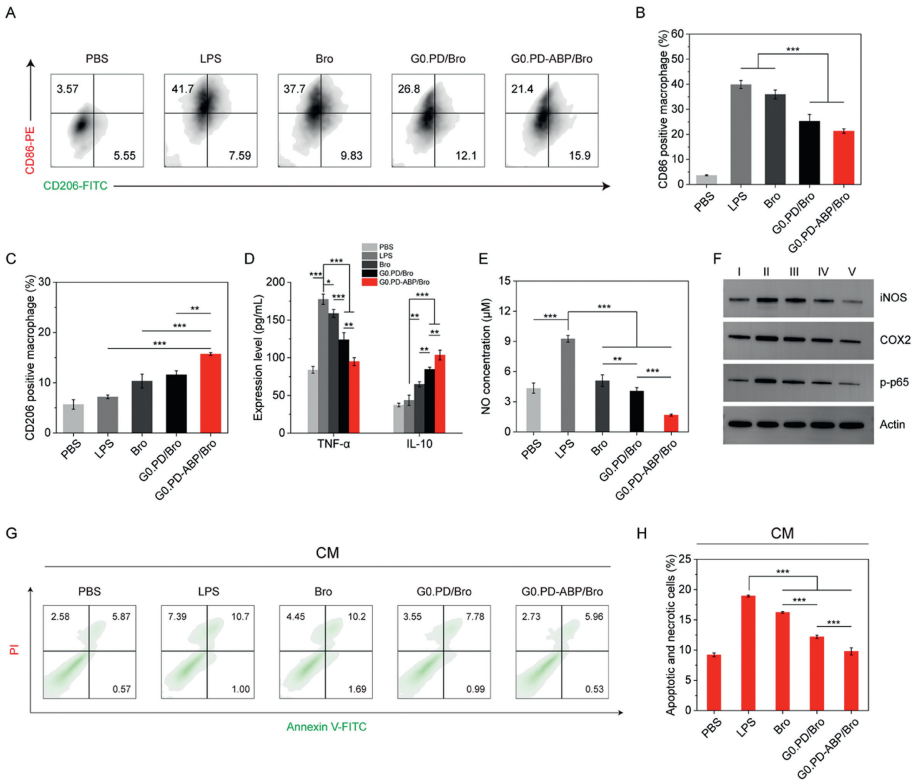


Fig. 3. Anti-inflammatory and chondroprotective ability of G0.PD-ABP/Bro NCs. (A) Representative flow cytometry plots of macrophage polarization after different treatments. The percentages of (B) CD86- and (C) CD206-positive macrophages after activated RAW264.7 cells were treated with different materials. (D) Enzyme-linked immunosorbent assay (ELISA) of the TNF-α and IL-10 secretion levels in the supernatants of macrophages following different treatments. (E) NO concentration of supernatants in macrophages treated with different materials. (F) Western blot analyses of iNOS, COX2, and p-p65 in macrophages treated with different materials. (G) Flow cytometry analyses and (H) quantitative results of apoptotic and necrotic chondrocytes after culturing with various culture media. For (F): I, PBS; II, LPS; III, Bro; IV, G0.PD/Bro; and V, G0.PD-ABP/Bro. Data are presented as mean ± standard deviation ($n = 3$). $^{*}P < 0.05$, $^{**}P < 0.01$, $^{***}P < 0.001$.

ing, and healthy mice display intact cartilage tissue with a uniform and deep glycosaminoglycan staining (red). Conversely, cartilage tissue in OA mice features multiple areas of light or absent staining, suggesting severe cartilage loss and glycosaminoglycan degradation occurred in the knee joints of OA mice (Fig. 4B). Due to the low bioavailability of Bro, the cartilage tissue of Bro treatment group still exhibits similar unreddened areas, similar to the OA group. Fortunately, G0.PD/Bro and G0.PD-ABP/Bro groups have noticeable anti-cartilage apoptotic capacity likely due to the synergistic effects of both dendrimers and Bro with improved intracellular delivery efficiency, in agreement with the *in vitro* results. Notably, the G0.PD-ABP/Bro exhibits a more prominent performance to ameliorate cartilage degradation than the G0.PD/Bro, as observed by the results of homogeneous staining of cartilage tissue with safranin O (a dye specific for cartilage binding) and the attainment of the lowest Osteoarthritis Research Society International (OARSI) score (Fig. 4B and Fig. S17 in Supporting information). Furthermore, terminal deoxynucleotidyl transferase dUTP nick end labeling (TUNEL) staining of inflamed joints provides additional evidence that G0/PD-ABP/Bro exhibits the strongest capacity to inhibit chondrocyte apoptosis among all materials studied ($P < 0.05$, Fig. S18 in Supporting information).

Consistently, immunofluorescence staining of MMP-13 shows increased positive expression in the articular cartilage of an OA mouse model. The G0.PD-ABP/Bro treatment diminishes the expression of MMP-13 in chondrocytes, which facilitates the blockade of ECM degradation to protect cartilage tissue integrity (Fig. 4C and Fig. S19 in Supporting information). To illustrate the progress of knee OA clearly after different interventions, the micro computed tomography (Micro-CT) images of the inflamed joint were collected at the end of treatment (Fig. 4D). Severe bone erosion and rough cartilage surfaces are observed in the OA group, which is opposed to the phosphate buffered saline (PBS) group. Fortunately, the degree of bone and cartilage restoration is significantly improved in the G0.PD-ABP/Bro group, whereas the improvement in the G0.PD/Bro group is fairly limited, confirming the benefit of enhanced Bro delivery in alleviating bone erosion. The bone mineral density (BMD), bone volume fraction (BV/TV), and trabecular thickness (Tb.Th) were measured to evaluate microstructure changes of the subchondral bone. As depicted in Figs. 4E–G, treatment with G0.PD-ABP/Bro results in a remarkable elevation in BV/TV (from 31.4 % to 46.2 %), BMD (from 0.4 g/cm^3 to 0.6 g/cm^3), and Tb.Th (from 0.08 mm to 0.1 mm) compared to OA mice, surpassing the results of the G0.PD/Bro-treated group in terms of improvement in BV/TV and BMD indices ($P < 0.05$). This further suggests that the G0.PD-ABP/Bro reestablishes homeostasis between bone metabolism and bone synthesis within the damaged joints by improving the bioavailability of Bro and synergizing the immune activity of dendrimers.

Encouraged by the robust macrophage M2 polarization property of the G0.PD-ABP/Bro NCs *in vitro*, we subsequently investigated the effect of the NCs on macrophage phenotype in synovial regions of inflamed joints. In Fig. 5A, intense iNOS positive expression in the OA group implies that synovial macrophages are successfully polarized to an M1 phenotype, which is detrimental to cartilage repair and inflammatory abatement. Although free Bro treatment is effective in reducing iNOS expression to some extent but has limited ability to enhance CD206 expression of synovial macrophages. Given that G0.PD and G0.PD-ABP enhance the intracellular Bro delivery while simultaneously modulating the macrophage phe-

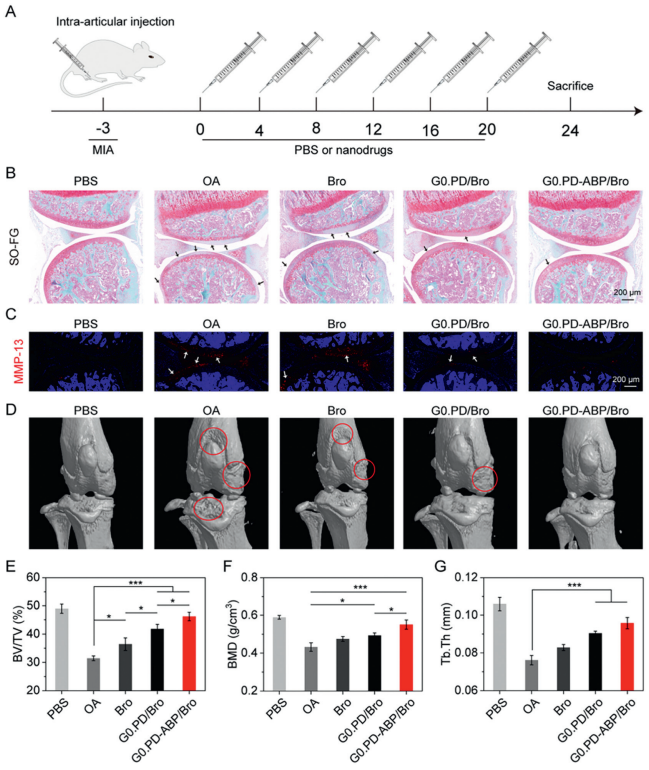


Fig. 4. Evaluation of *in vivo* therapeutic efficacy of G0.PD-ABP/Bro. (A) Schematic illustration of the establishment of the OA mouse model and the experimental design. MIA, sodium iodoacetate. Representative (B) SO-FG and (C) MMP-13 staining of the knee joint in OA mice after different interventions (black arrows indicate cartilage tissue with light or absent SO-FG staining, and white arrows indicate cartilage tissue with MMP-13 positive expression). (D) Representative Micro-CT images of inflamed joint in OA mice after different treatments (Red circles represent bone erosion areas or rough chondrocyte surfaces). Quantitative results of (E) BV/TV, (F) BMD, and (G) Tb.Th of subchondral bone. Data are presented as mean ± standard deviation ($n = 3$). $^{*}P < 0.05$, $^{***}P < 0.001$.

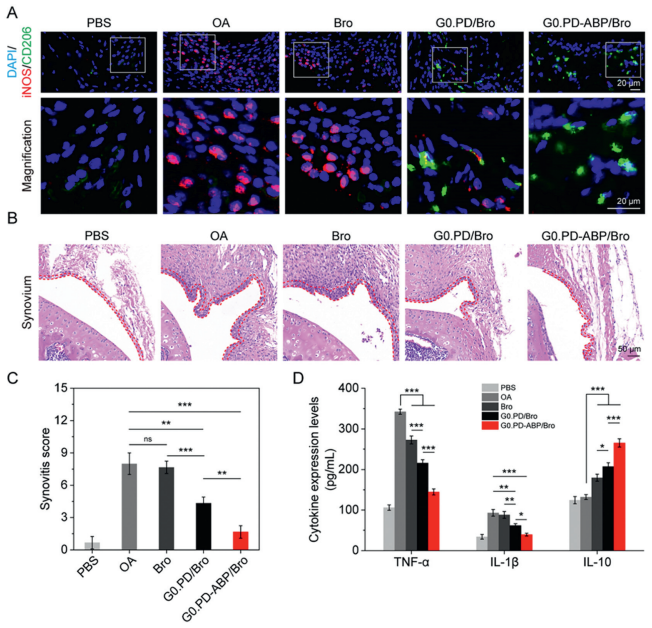


Fig. 5. Evaluation of *in vivo* anti-inflammatory therapeutic effects of G0.PD-ABP/Bro. (A) Representative immunofluorescence staining of iNOS and CD206 expressions in the knee joint of OA mice received different treatments. (B) Representative H&E staining images of the synovium tissue in OA mice received different treatments. (C) Synovitis score of various treatments based on the H&E staining results (dashed areas are synovial tissue). (D) Expression levels of TNF-α, IL-1β, and IL-10 in the serum of OA mice after various treatments. Data are presented as mean ± standard deviation ($n = 3$). $^{*}P < 0.05$, $^{**}P < 0.01$, $^{***}P < 0.001$.

notype, both G0.PD/Bro and G0.PD-ABP/Bro exhibit much better efficacy than free Bro in promoting M2 polarization of synovial macrophage phenotype ($P < 0.001$, Fig. S20A in Supporting information). Remarkably, the superior intracellular delivery of Bro by asymmetric phosphorus dendrimer G0.PD-ABP than the symmetric G0.PD enables the augmented activation of CD206 expression in the G0.PD-ABP/Bro group (Fig. S20B in Supporting information). This is quite different from the *in vitro* data showing that there is no significant difference between free phosphorus dendrimers in terms of their ability to exert anti-inflammation and macrophage polarization efficacy.

Synovitis is an important feature of OA. Hematoxylin and eosin (H&E) staining reveals that treatment with G0.PD-ABP/Bro ameliorates the symptoms of synovitis at the inflamed joint site including reduced hypertrophy and hyperplasia of the synovium, decreased thickness of the synovial lining cell layer, as well as inhibited infiltration of inflammatory cells (Fig. 5B). In addition, the excellent macrophage M2 polarization property of G0.PD-ABP/Bro results in a significant decrease in synovitis scores (Fig. 5C), which should be attributed to the ability of NCs to downregulate various proinflammatory cytokines (TNF-α and IL-1β) and upregulate anti-inflammatory cytokine (IL-10) mediated by the M2 macrophages (Fig. 5D). Taken together, the G0.PD-ABP/Bro NCs can achieve outstanding anti-inflammatory therapeutic effects by polarizing synovial macrophages towards M2 phenotype and modulating the expression of inflammatory cytokines in an OA mouse model.

Ultimately, the biosafety of the G0.PD-ABP/Bro NCs was evaluated by monitoring the body weight changes of mice, H&E staining of major organs, and blood routine and serum biochemical assays. As illustrated in Fig. S21 (Supporting information), all treatment groups exhibit a similar trend in weight gain as the PBS group. After different treatments, the G0.PD-ABP/Bro and PBS groups show the normal range of various hematological parameters and the levels of alanine transaminase (ALT), aspartate transaminase (AST), triglyceride (TG), and uric acid (UA) (Fig. S22 in Supporting information) [14,15]. Notably, the serum TG and UA levels in the G0.PD-ABP/Bro group are lower than those in the PBS group. This disparity can potentially be ascribed to individual differences among different mice or the nanomaterial-mediated attenuation of systemic inflammatory response. Such anti-inflammatory characteristic may influence inflammation-driven lipid metabolism and uric acid production, thereby reducing TG and UA levels [41,42]. Additionally, the G0.PD-ABP/Bro treatment causes negligible damage or inflammation in the main organs of the experimental mice. These results collectively confirm the excellent *in vivo* biosafety of the G0.PD-ABP/Bro NCs (Fig. S23 in Supporting information).

In summary, we developed bioactive asymmetric phosphorus dendrimers (G0.PD-ABP)/Bro NCs for intracellular Bro delivery to restore inflammation and cartilage homeostasis in OA. Although the structural symmetry of phosphorus dendrimers does not potentiate their capacity to regulate macrophage polarization or inflammatory cytokine mRNA expression, the asymmetric G0.PD-ABP exhibits superior Bro delivery efficiency compared to symmetric one. Such G0.PD-ABP-enhanced intracellular Bro delivery augments the inhibitory effect of Bro on multiple inflammatory signaling pathways and induces macrophage polarization towards an anti-inflammatory M2 phenotype by synergizing with the intrinsic immunomodulatory activity of the phosphorus dendrimer. The potent anti-inflammatory activity of G0.PD-ABP/Bro NCs leads to excellent synovitis-relieving therapeutic effects, reestablishing homeostasis between cartilage anabolism and catabolism in an OA mouse model.

Declaration of competing interest

The authors declare that they have no known competing financial interests or personal relationships that could have appeared to influence the work reported in this paper.

CRediT authorship contribution statement

Huxiao Sun: Writing – original draft, Visualization, Validation, Methodology, Investigation, Formal analysis, Data curation. **Jin Li:** Writing – original draft, Visualization, Validation, Methodology, Investigation, Formal analysis, Data curation. **Mengsi Zhan:** Investigation, Formal analysis, Data curation. **Yu Zou:** Writing – review & editing, Supervision, Project administration. **Caiyun Zhang:** Formal analysis, Data curation. **Serge Mignani:** Supervision, Project administration. **Regis Laurent:** Supervision, Project administration. **Jean-Pierre Majoral:** Supervision, Resources, Project administration, Funding acquisition. **Xiangyang Shi:** Writing – review & editing, Supervision, Resources, Project administration, Funding acquisition, Conceptualization. **Mingwu Shen:** Writing – review & editing, Supervision, Resources, Project administration, Funding acquisition, Conceptualization.

Acknowledgments

This research is financially supported by the National Key R&D Program (No. 2024YFE0108100), the China-Central and Eastern European Countries (CEEC) Joint Education Project (No. 2023256), the National Natural Science Foundation of China (Nos. U23A2096 and 52350710203), the Science and Technology Commission of Shanghai Municipality (Nos. 23520712500 and 20DZ2254900), and the Fundamental Research Funds for the Central Universities and Graduate Student Innovation Fund of Donghua University (No. CUSF-DH-D-2024038). Scheme 1 and graphical abstract were created by BioRender.com.

Supplementary materials

Supplementary material associated with this article can be found, in the online version, at doi:10.1016/j.cclet.2025.111446.

References

[1] H. Lu, J. Wei, K. Liu, et al., ACS Nano 17 (2023) 6131–6146.
[2] Z. Li, H. Lu, L. Fan, et al., Adv. Sci. 11 (2024) 2406942.
[3] G. Li, S. Liu, Y. Chen, et al., Nat. Commun. 14 (2023) 3159.
[4] X. Gao, L. Yan, W. Zhang, et al., Nano Today 53 (2023) 102047.
[5] C. Xie, Q. Sun, Y. Dong, et al., ACS Nano 17 (2023) 12842–12861.
[6] R. Deng, R. Zhao, Z. Zhang, et al., Sci. Transl. Med. 16 (2024) eadh9751.
[7] P. Chen, X. Liu, C. Gu, et al., Nature 612 (2022) 546–554.
[8] X. Song, L. Gu, Q. Yang, et al., Chin. Chem. Lett. 34 (2023) 108079.
[9] S.H. Cui, Y. Yan, A. Lu, et al., ACS Nano 18 (2024) 8125–8142.
[10] X. He, S. He, G. Xiang, et al., Adv. Mater. 36 (2024) 2405943.
[11] K. Zhou, C. Yang, K. Shi, et al., Biomaterials 295 (2023) 122036.
[12] Z. Zhou, F. Gong, P. Zhang, et al., Nano Res. 15 (2022) 3338–3345.
[13] P. Wojdasiewicz, Ł.A. Poniatowski, D. Szukiewicz, Mediat Inflamm. (2014) 561459 2014.
[14] M. Zhan, H. Sun, Z. Wang, et al., ACS Nano 18 (2024) 10625–10641.
[15] H. Sun, M. Zhan, Y. Zou, et al., Biomaterials 316 (2025) 122999.
[16] V. Kumar, B. Mangla, S. Javed, et al., Food Funct. 14 (2023) 8101–8128.
[17] O. Insuan, P. Janchai, B. Thongchuai, et al., Curr. Issues Mol. Biol. 43 (2021) 93–106.
[18] J.R. Huang, C.C. Wu, R.C.W. Hou, et al., Immunol. Invest. 37 (2008) 263–277.
[19] L. Chen, H. Wang, Y. Cheng, Chin. Chem. Lett. 37 (2026) 111172.
[20] S. Guo, H. Xu, Z. Cheng, et al., Chin. Chem. Lett. 36 (2025) 111022.
[21] F. Hu, J. Qi, Y. Lu, et al., Chin. Chem. Lett. 34 (2023) 108250.
[22] J. Xu, Z. Li, Q. Fan, et al., Adv. Mater. 33 (2021) 2104355.
[23] K. Liang, S. Ng, F. Lee, et al., Acta Biomater. 33 (2016) 142–152.
[24] L. Shi, W. Wu, Y. Duan, et al., Angew. Chem. Int. Ed. 59 (2020) 19168–19174.
[25] J.E. Chung, S. Tan, S.J. Gao, et al., Nat. Nanotechnol. 9 (2014) 907–912.
[26] H. Sun, M. Zhan, A. Karpus, et al., ACS Nano 18 (2024) 2195–2209.
[27] Y. Peng, M. Zhan, A. Karpus, et al., ACS Nano 18 (2024) 10142–10155.
[28] J. Ma, M. Zhan, H. Sun, et al., Adv. Healthc. Mater. 13 (2024) 2401462.
[29] Y. Zou, S. Shen, A. Karpus, et al., Biomacromolecules 25 (2024) 1171–1179.
[30] M. Hayder, M. Poupot, M. Baron, et al., Sci. Transl. Med. 3 (2011) 81ra35.
[31] A.K. Sarkar, K. Debnath, H. Arora, et al., ACS Appl. Mater. Interfaces 14 (2022) 3199–3206.
[32] H. Chang, J. Lv, X. Gao, et al., Nano Lett. 17 (2017) 1678–1684.
[33] D. Prozeller, S. Morsbach, K. Landfester, Nanoscale 11 (2019) 19265–19273.
[34] M. Braia, D. Loureiro, G. Tubio, et al., Colloids Surf. B 155 (2017) 507–511.
[35] C. Huo, G. Liu, M. Xu, et al., Spectrochim. Acta Part A 263 (2021) 120213.
[36] X. Yang, M. Tan, J. Guo, et al., Adv. Funct. Mater. 34 (2024) 2401963.
[37] F. Zhou, J. Mei, S. Yang, et al., ACS Appl. Mater. Interfaces 12 (2020) 2009–2022.
[38] S.K. Bedingfield, J.M. Colazo, F. Yu, et al., Nat. Biomed. Eng. 5 (2021) 1069–1083.
[39] J. Li, L. Chen, C. Li, et al., Theranostics 12 (2022) 3407–3419.
[40] J. Yin, H. Zeng, K. Fan, et al., Cell Death Dis. 13 (2022) 567.
[41] H. Wang, S.e. Su, X. An, et al., Bioact. Mater. 45 (2025) 496–508.
[42] M. Chen, J. Luo, H. Ji, et al., J. Funct. Foods 110 (2023) 105863.